國立交通大學

材料科學與工程學系奈米科技碩士班

碩士論文

奈米點陣列的尺寸對神經膠細胞調控神經細胞增生的影響

The sizes of nanodot array influence glial regulation on neuronal proliferation .

研 究 生: 黃秋淵

學 號 ： 9852517

指導教授: 黃國華 教授

中 華 民 國 一百 年 七 月

國立交通大學

材料科學與工程學系奈米科技碩士班

碩士論文

奈米點陣列的尺寸對神經膠細胞調控神經細胞增生的影響

The sizes of nanodot array influence glial regulation on neuronal proliferation .

研 究 生: 黃秋淵

學 號 ： 9852517

指導教授: 黃國華 教授

中 華 民 國 一百 年 七 月

奈米點陣列的尺寸對神經膠細胞調控神經細胞增生的影響

The sizes of nanodot array influence glial regulation on neuronal proliferation .

研 究 生:黃秋淵　　Student: Chiu –Yuan Huang

指導教授:黃國華　　Advisor: Dr. Guewha Steven Huang

國 立 交 通 大 學

材料科學與工程學系奈米科技碩士班

碩 士 論 文

A Thesis
Submitted to Graduate Program for Nanotechnology
Department of Materials Science and Engineering
College of Engineering
National Chiao Tung University
in partial Fulfillment of the Requirements
for the Degree of
Master
in

Nanotechnology

July 2011

Hsinchu, Taiwan, Republic of China

中華民國一百年七月

The sizes of nanodot array influence glial regulation on neuronal proliferation .

Student: Chiu-Yuan Huang Advisor: Dr. Guewha Steven Huang

Institute of Material Science and Engineering Graduate Program For Nanotechnology

National Chaio Tung University

Abstract

Traditionally regarded as supporting cells, glia cells are structurally and functionally poised as ideal sensors and regulators of local microenvironments. Emerging evidence suggests that glia have key roles in regulating neuronal development. The differentiated type of neuroblastoma glioma hybrid cell line, NG108-15, has widely used in in vitro studies instead of primary-cultured neurons. We culture NG108-15 cells on different sizes of nanodot arrays to examine how glia cells sense nanoenvironment stimulis and regulate neuronal development. Here we show that different nanodot size arrays change the number of neuroblastoma cells on unit area of glioma cells. Our results show that glia can sense nanoenvironment stimulis and response in different regulation of neuronal development. By examining gene expression, nanodot sizes also influence glia-mediated neuronal factor, such as Wnt3 and BDNF. Our results show that glia can sense nanoenvironment stimulis and response in different regulation of neuronal development. The nanodot arrays can serve as an appropriate tool for investigating glia-neuron interactions.

致　謝

不知不覺，又到了畢業的時節。從大學開始，送走了不少畢業生，如今換我穿上畢業服，準備走出校園開始一趟新的旅程。在交大待了兩千多個日子，在此有許多回憶，或開心，或痛苦，隨著不同時期的回憶層層堆疊，每當我走過校園每一個角落時都會有很深的感動。

不同於大學時期，研究所的實驗室生涯是比較苦悶的，窩在圖書館讀論文、到處奔波做實驗或是為了趕進度而徹夜未眠。有人說”研究生不死，只是生不如死”，雖然實際生活沒那麼誇張，但看到這句話總不禁會心一笑。幸好在實驗室裡有許多夥伴，總是在我低潮的時候鼓勵、幫助我，讓實驗生活添了不少樂趣。

在這兩年的時間裡，我學到許多。當初從材料背景跨到生物領域，一開始讓我吃了不少苦頭，但也讓我之後對於學習跨領域的東西更有信心。尤其在研究所學習的東西是零碎的，不像大學有系統的教學課程，我們必須自行將學到的知識整合，並勾勒出系統架構，這樣的訓練讓我在自學其他才藝上無往不利。很感謝老師在我碩一時帶我去俄羅斯進行實驗室交流，那段時間老師的口才訓練改善了我長久以來最不擅長的上台呈現，雖然那段時間很掙扎，但學到了很紮實的英文簡報技巧。在碩一升碩二的那年暑假遇到實驗瓶頸，原本做得好好的神經實驗卻突然連續兩三個月都不成功，仔細檢視、改善各樣實驗步驟卻都依舊徒勞，在那段時間，我學會如何在撞牆期自處。有很多事情別人只能給你建議或陪你走一小段路，但最終還是要自己去處理、面對。學習如何和孤單相處；學習如何獨立；學習如何和別人合作、協調，在這說長不長說短也不短的兩年內有太多事情要學習，而我們也變得更成熟。

一路走來，要感謝的人太多了。感謝老師的諄諄教誨和督促，讓我們在這兩年有充足的學習，不僅在課業上，更在待人處世的道理上有深刻的體悟。感謝師母無微不至的照顧與叮嚀，讓我們出門在外仍能感受到溫暖。感謝實驗室的博班學姐不厭其煩地指導我們做實驗並包容我的幼稚。感謝同屆一起奮鬥的夥伴，永遠記得那些一同做實驗、彼此掩護的日子。也感謝學弟妹不時提供的幫助和鼓勵。感謝我的家人，因為他們無怨無悔的支持和奉獻我才能夠無後顧之憂地就讀研究所。最後我要感謝上帝，因祂對我生命的安排實在奇妙，當初在當兵和研究所之間猶豫許久，而祂帶領我來到這裡，讓我接受許多的操練並成長，衷心地感謝主。

Contents ……III

1. Introduction.....1

2. Materials and methods.....3

2.1 Fabrication of the nanodevice/matrix of nanodot arrays.....3

2.2 Cell culture.....3

2.3 Scanning electron microscopy.....3

2.4 Immunostaining of vinculin and phalloidin.....4

2.5 Statistics.....5

3. Result and discussion.....7

3.1 Fabrication of an integrated nanodot array device.....7

3.2 Different morphological changes of NG108-15 on nanodot arrays.....7

3.3 The sizes of nanodot influence glia-neuron interaction.....8

3.4 The sizes of nanodot array also influence processes of glioma cells.....9

4. Conclusion.....11

Reference.....20

List of Figures

Figure 1…….. 12

Fabrication of different sizes of nanodot arrays.

Figure 2……. …….13

SEM images of NG108-15 cells on different sizes of nanodot arrays

Figure 3. …….14

(A) Area of Glioma on day 1. (B) The number of neuroblastoma cells divided by the area of glioma cells on day 1. (C) Area of Glioma on day 2. (D) The number of neuroblastoma cells divided by the area of glioma cells on day 2

Figure 4……..15

Filopodia of neuroblastoma cells on nanodot arrays on day 2

Figure 5……..16

(A) Filopodia numbers of neuroblastoma cell (B) Perimeter of neuroblastoma (C) Filopodia number of neuroblastoma divided by perimeter (D) Filopodia length of neuroblastoma

Figure 6……..18

Confocal images of NG108-15 cells on different nanodat arrays.

Figure 7……..18

Percentage of glioma processes number distribution range on different sizes nanodot arrays.

Figure 8……..... 19

Fold change of each gene. We use GAPDH and flat surface as our control.

1. Introduction

The nervous system plays a leading role in the body; it controls and regulates the various activities of the body organs to maintain the relative balance of the body with the internal and external environments(*1*) . Damage to the nervous system can result in lack of body organ function and related diseases, such as Alzheimer's disease, Parkinson's disease, depressive disorder, and reduced reproductive functions (*2-6*). To date, considerable effort has been focused on the development of new techniques and studies involving the molecular and cellular mechanisms that influence axonal plasticity and response to injury(*7*) . However, in contrast to the ability to treat peripheral nerve injury, there is no current treatment capable of completely restoring functions after central nervous system injury. Generally, the current medical treatments achieve limited success in restoring functions and regeneration for severely injured nerves(*8*).

Traditionally regarded as supporting cells, glia cells are abundant in the adult CNS and structurally and functionally poised as ideal sensors and regulators of local microenvironments(*9*). Emerging evidence suggests that glia cells perform a much wider range of functions than previously appreciated, such as regulation of axon guidance, synapse formation and plasticity(*9, 10*). Moreover, glia cells promote neuronal proliferation(*11, 12*). This provides a way to regulate neuronal regeneration by giving various stimuli to glia cells.

Biomechanical cues can be transmitted to cell via micro or nanoscale substrate topography(*13-21*). Morphological and functional changes have been observed for various types of cells, including glia cells(*22, 23*), when cultured on substrates presenting topographical features such as pillars and grooves(*24-27*). In addition, these changes were regulated in a size-dependent manner(*28, 29*). We are interested in

the question of whether one can use topography-induced glia-neuron interactions to control neuronal proliferation.

In this study, we fabricated a nanodevice consisting of a matrix of nine nanodot arrays with various dot sizes ranging from a flat surface to 200 nm dots(*30*). We cultured NG108-15 cells, a hybrid cell line of mouse neuroblastoma and rat glioma, on the nanodot arrays to investigate how the sizes of nanodot arrays influence glia-mediated proliferation of neurons. We examined the morphological changes and gen expression of cells on different sizes of nanodot arrays.

2. Materials and methods

2.1 Fabrication of the nanodevice/matrix of nanodot arrays

Nanodot arrays were fabricated as described(*31*). A tantalum nitride (TaN) thin film with a 200 nm thickness was deposited onto a 6 in silicon wafer followed by deposition of 400 nm thick aluminium on top of the TaN layer. Anodization was carried out in 1.8 M sulfuric acid at 5 V for the 10 nm nanodot array, and in 0.3 M oxalic acid at 25 V and 100 V for the 50 nm and 100 nm nanodot arrays or in 5% (w/v) phosphate acid (H_3PO_4) at 100 V for 200 nm nanodot arrays. Porous anodic alumina was formed during the anodic oxidation. The underlying TaN layer was oxidized into tantalum oxide nanodots using the alumina nanopores as a template. The porous alumina was removed by immersion in 5% (w/v) H_3PO_4 overnight. A thin layer of platinum (ca. 5 nm) was sputtered onto the structure to improve biocompatibility and to unify the surface chemistry. The dimensions and homogeneity of the nanodot arrays were measured and calculated from images taken using JEOL JSM- 6500 TFE-scanning electron microscopy (SEM).

2.2 Cell culture

NG108-15 cells were cultured in high glucose-containing Dulbecco's Modified Eagle's Medium supplemented with 0.1 mM hypoxanthine, 1 μM aminopterin, 16 μM thymidine, 50 U/mL penicillin, and 10% FBS. The cells were harvested and reseeded at a density of 1 *10^5/mL in 6 wells, filled with 2 mL of the above medium.

2.3 Scanning electron microscopy

Harvested cells were fixed with 1% glutaraldehyde in phosphate buffered saline

(PBS) at 4 ˚C for 20 min, followed by post-fixation in 1% osmium tetroxide for 30 min. Dehydration was performed through a series of ethanol concentrations (5 min incubation each in 50%, 60%, 70%, 80%, 90%, 95%, and 100% ethanol) followed by air drying. The specimens were sputtercoated with platinum and examined by JEOL JSM-6500 TFESEM at an accelerating voltage of 10 keV. We randomly picked six SEM pictures for each condition, and we calculated the number of abnormal cells and the total number of cells.

2.4 Immunostaining of vinculin and phalloidin

Cells were harvested and fixed with 4% paraformaldehyde in PBS for 15 min, followed by three washes in PBS. The membrane was permeabilized by incubation in 0.1% Triton X-100 for 10 min. Permeabilization was followed by three PBS washes, blocking with 1% bovine serum albumin (BSA) in PBS for 1 h, and three washes in PBS. The sample was incubated with anti-vinculin antibody (properly diluted in 0.5% BSA) and phalloidin for 1 h, followed by incubation with Alexa Fluor 488 goat anti-mouse antibody for 1 h, followed by three washes in PBS. We randomly picked 100 fluorescent cells for each condition and calculated the processes of glioma cells.

2.5 RT-PCR

Reverse-Transcription PCR and Real-Time Reverse-Transcription PCR Analysis. Analysis was performed using the following oligonucleotide primers : Wnt3 , Frizzled 1 , β- catenin(L) , β- catenin(S) , BDNF , GFAP . We used GAPDH as control. Primers are listed in Table 1.

The PCR program consisted of initial denaturation at 95°C for 30 seconds, annealing at temperatures suggested by data sheet for 40 seconds, and extension at

72°C for 30 seconds for 25-30 cycles. Specificity of all PCR reactions was tested via parallel reactions using water instead of cDNA . The PCR products were subjected to 1% agarose gel electrophoresis and visualized via ethidium bromide.

Gene	Primer sequences
Wnt3	F : 5'- GCCTCTGACAAGCCCGAAA - 3'
	R: 5'- GCGACGCCCCCAATAGTT -3'
β-catenin(L)	F: 5'- GCTGACCTGATGGAGTTGGA -3'
	R: 5'- GCTACTTGCTCTTGCGTGAA -3'
β-catenin(S)	F: 5'- GCTGACCTGATGGAGTTGGA -3'
	R: 5'- TCTTCTTCTCAGGATTGCC -3'
Frizzled 1	F: 5'- GCGCACCTGGATAGGCAT -3'
	R: 5'- TACTAGGTACGTGAGCACCGTGA-3'
BDNF	F: 5'- CGTGATCGAGGAGCTGTTGG -3'
	R: 5'- CTGCTTCAGTTGGCCTTTCG -3'
GFAP	F: 5'- CAAGCCAGACCTCACAGCG -3'
	R: 5'- GGTGTCCAGGCTGGTTTCTC -3'
GAPDH	F: 5'- CCTGCACCACCAACTGCTTAGC -3'
	R: 5'- GCCAGTGAGCTTCCCGTTCAGC -3'

Table 1. The gene-specific primers used for real time-PCR.

2.5 Statistics

Throughout, student's t-test (for two samples, assuming unequal variances) was used to compare statistical significance of test materials against the control. Results

of p <0.05 were considered significant (differences p<0.05 denoted by * , p<0.01 denoted by **).

3. Result and discussion

3.1 Fabrication of an integrated nanodot array device

Nanodot arrays with dot sizes range from 10 nm to 200 nm (Fig. 1). Nanodot arrays were fabricated by AAO processing on a tantalum-coated wafer.26 Tantalum oxide nanodot arrays with dot diameters of 10 nm, 50 nm, 100 nm, and 200 nm were constructed using different solutions and voltages on a silicon wafer. To provide a biocompatible and unique interaction surface, platinum of ca. 5 nm thickness was sputter-coated onto the top of the nanodots. SEM showed diameters of 10* 2.8 nm,52* 5.6 nm, 102 * 9.2 nm, and 212 * 18.6 nm for 10 nm, 50 nm, 100 nm, and 200 nm dot arrays, respectively . The dimensions of the nanodots were well-controlled and highly defined.

3.2 Different morphological changes of NG108-15 on nanodot arrays

SEM examination of NG108-15 cell morphology following cell seeding on different sizes of nanodot arrays revealed that nanoscale topography influenced cell morphology (Fig. 2). We measure the area of glioma (Fig. 3A and 3C) and the ratio of the neuroblastoma numbers divided by the area of glioma (Fig. 3B and 3D). The area of glioma represents the viability of glioma. On day1, glioma grows well on glass and 100nm, but on other surfaces, glioma shows no specific distribution. On day2, we can see nanotopography really inhibit glioma growth, and the tendency remains unchanged.

The ratio of the neuroblastoma numbers / the area of glioma also showed no apparent trend between glia – neuron interaction on day 1. On day 2, the ratio of 50nm nanodot arrays is significantly higher than other surface. This result indicates

50nm nanodot can promote neuronal proliferation by stimulating glioma cells. This tendency is similar to our previous research.

3.3 The sizes of nanodot influence glia-neuron interaction

We measure the perimeter of each neuroblastoma and calculate the filopodia numbers and length (Fig. 4). The tendency of filopodia length is similar to the ratio of the neuroblastoma numbers / the area of glioma, which shows that 50nm nanodot array has significant effect (Fig. 5). 50nm nanodot array also promote the filopodia formation, this suggest influences cellular motility, and also give us a new insight into the guide of cell and axonal growth cone migration. Individual filopodia can behave independently within one neuronal growth cone and contact of a single filopodium with an appropriate target is sufficient to induce a growth cone to turn . Actin polymerization occurs at the tip of a filopodium and regulating the rate of F-actin assembly has been proposed to be the dominant factor controlling the rate of filopodial extension in neuronal growth cones Since neuroblastoma cells grow on glioma, the 50nm nanodot array directly influences glioma, which then changes glia-mediated interaction with neuroblastoma.

3.4 The sizes of nanodot array also influence processes of glioma cells

Glioma can be stained by phalloidin, thus we can count the processes of glioma cells (Fig. 6). We counted the number of processes and set the range of numcers into several groups, for example, we put cells that have 0~2 processes into a group, then 3~5, 6~8, 9 and more (Fig. 7). We found that glioma cells have less processes on 10nm, 50nm and 100nm nanodot arrays, especially 50nm. Glioma cells on 200nm nanodot array have similar distribution of process numbers with flat surface.

More processes can enhance the ability of cells to explore the local environment and guide the direction of processes extension. Formation of highly ramified processes indicates maturation of glioma cells. The number of glioma cell process significantly decreased in cells on 10nm, 50nm and 100nm nanodot surfaceas compared with cells on flat and 200nm surfaces.

3.5 The gene expression of glioma cells that influences neuronal proliferation.

We now want to examine the mechanism of neuronal proliferation caused by glioma cells since nanodot arrays affected glioma cells directly. From previous studies, Wnt3 is known for its neurogenesis ability, thus we choosed the related pathway of Wnt3(*32-34*), including β-catenin(L) , β-catenin(S) , and Frizzled 1, which is the inhibitor of Wnt3. We also choosed another neurogenesis factor – Brain-derived neurotrophic factor(BDNF)(*35-37*). Because glioma cells has directly contact with nanotopography, so we choosed GFAP to examine the characterization of glioma. GAPDH is used as our control. The genes above are all for rat.

The result of real-time PCR shows on the Fig.8 .We compared each size of nanodot arrays with flat surface and calculated the fold change of each gene.

Among the proliferation-related genes, only β-catenin(S) shows a similar trend as Fig.3D. Glioma cells on 50nm remained the same as flat surface, gene expression of other nanodot arrays significantly reduced. β-catenin(S) may be the key factor that affected glioma-induced neuronal proliferation through the stimuli of 50nm nanodot.

It is well known that expression of glial fibrillary acidic protein (GFAP) provided a phenotypic marker characteristic of astrocytes, which is induced by activation of intracellular signaling mechanisms that directly stimulate GFAP gene transcription. Althrough the morphology of glioma cells indicated that 50 nm were more immature, gene expression of GFAP showed an opposite result.

4. Conclusion

Different sizes of nanodot arrays have different influence on NG108-15 cells. The nanodot arrays affect neuroblastoma through glioma cells because only glioma cells directly contacted to surfaces. Although glioma on 50nm nanodot showed less maturation, the GFAP gene expression showed an opposite result. β-catenin(S) may be the key factor that induce significant neuroblastoma proliferation through glial regulation.

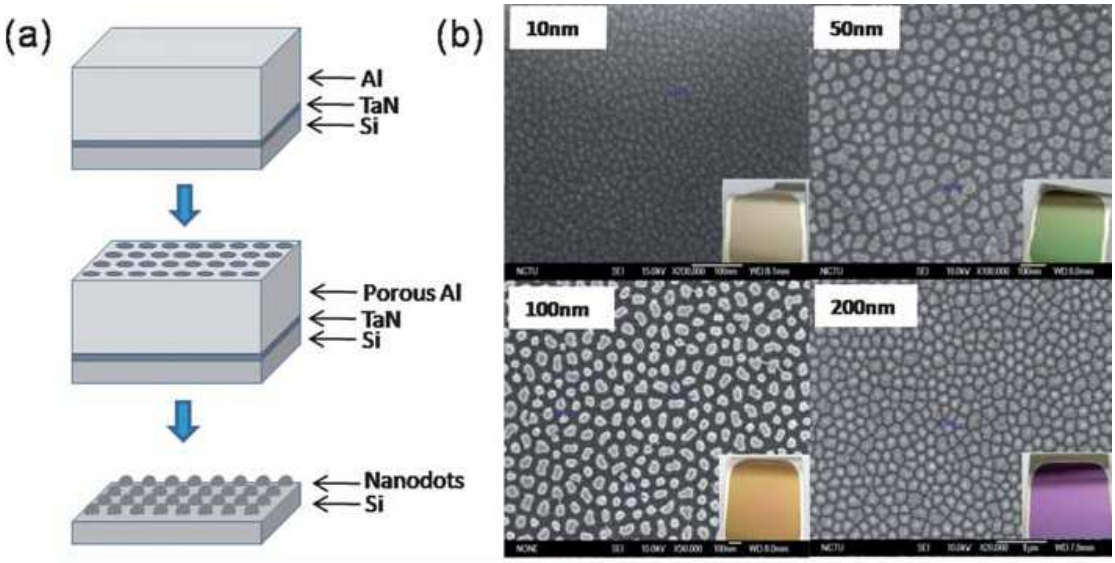

Fig. 1 Fabrication of different sizes of nanodot arrays. (a) Schematic representation of fabrication of tantalum-based nanodot arrays using AAO processing. (b) SEM images of tantalum oxide nanodot arrays with dot diameters of 10 nm, 50 nm, 100 nm, and 200 nm constructed on a silicon wafer.

	Day 1	Day2
Glass	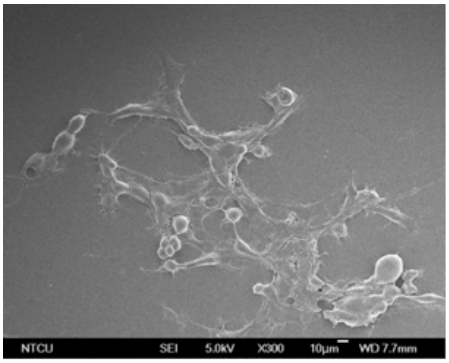	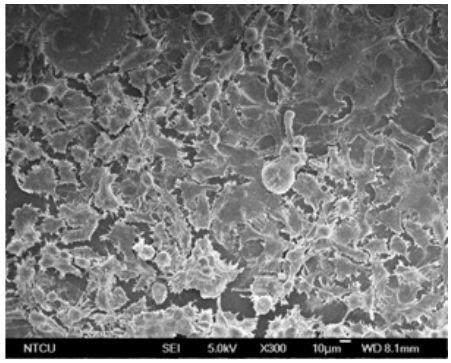
Flat	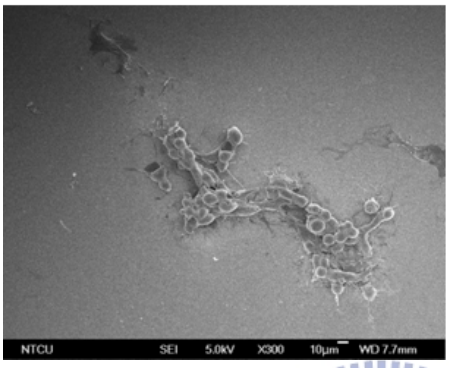	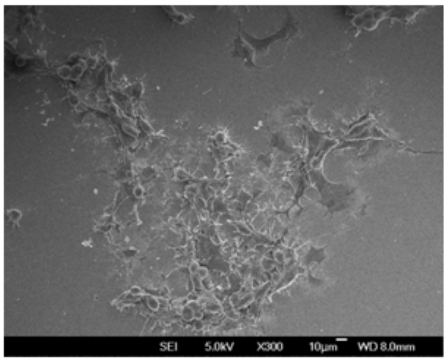
10nm	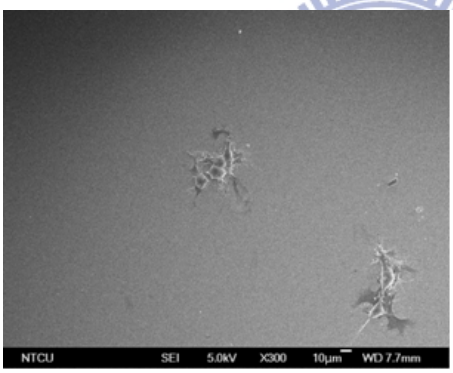	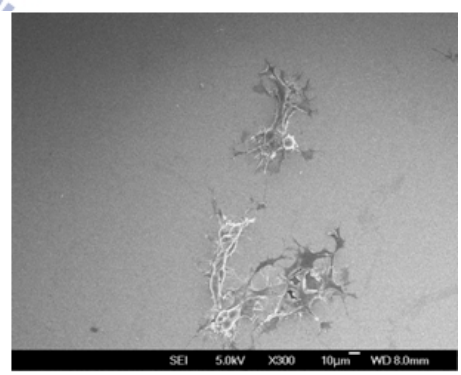
50nm	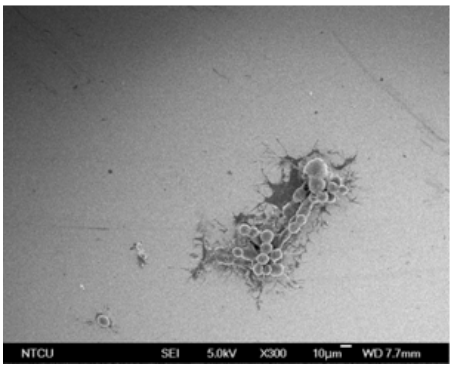	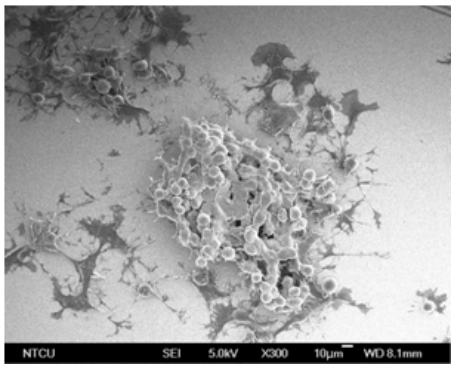

100nm

200nm

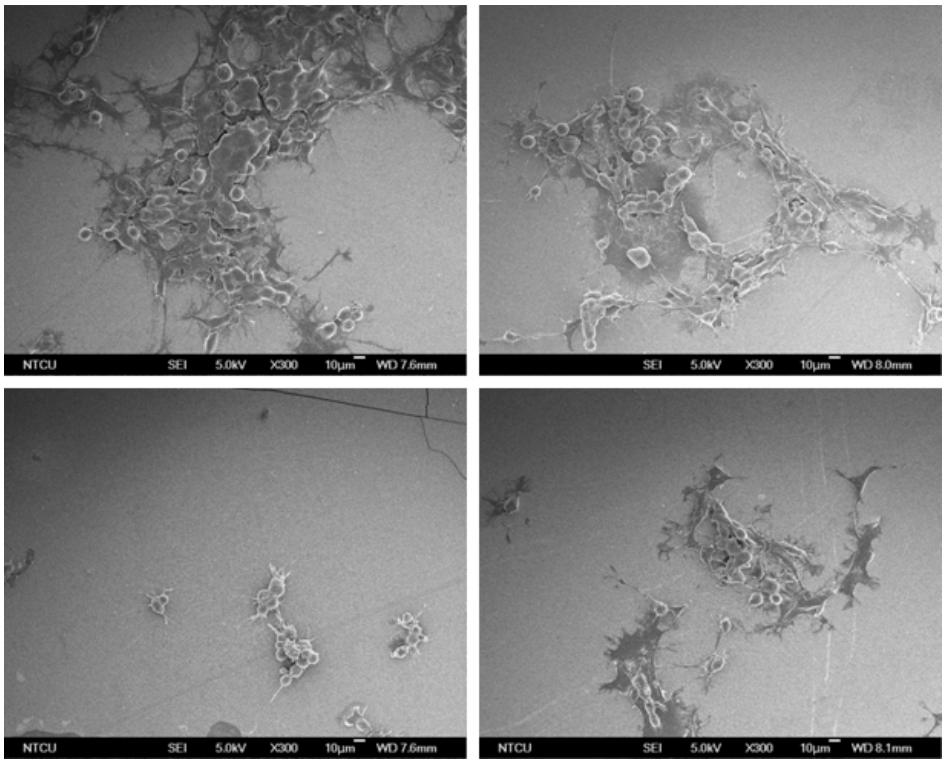

Figure 2. SEM images of NG108-15 cells on different sizes of nanodot arrays, we cultured cells for 1 day and 2 da

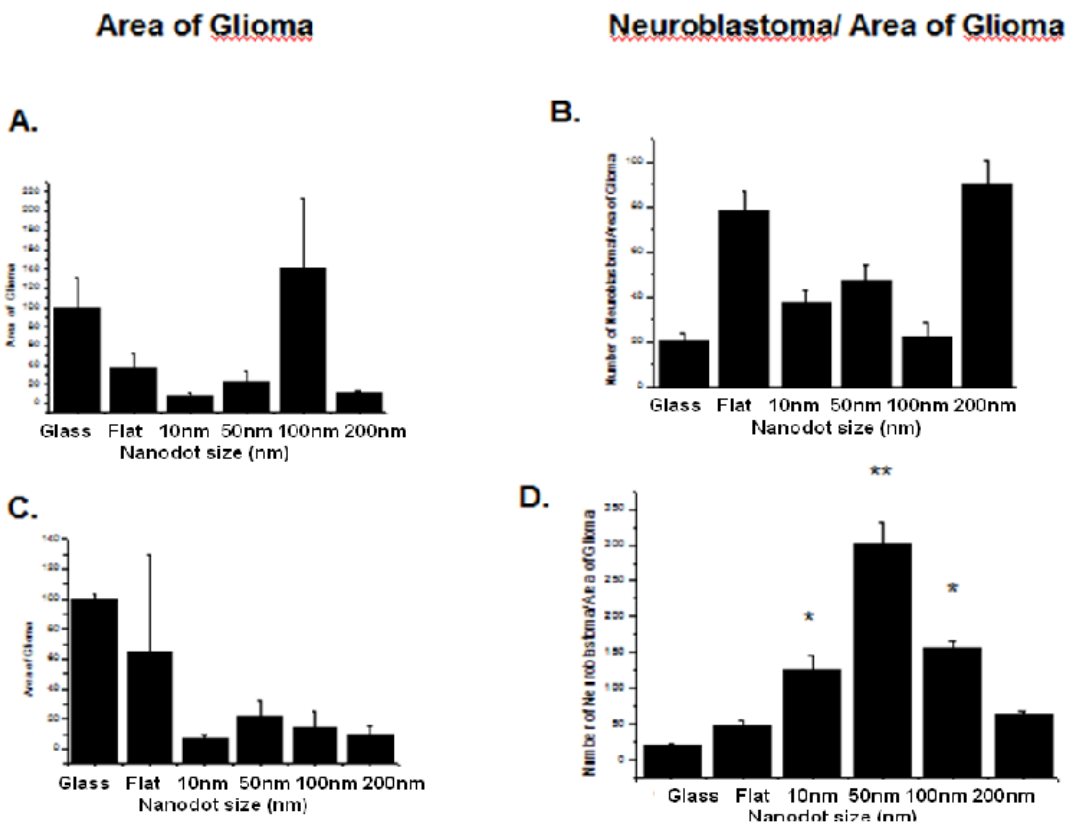

Figure3. (A) Area of Glioma on day 1. (B) The number of neuroblastoma cells divided by the area of glioma cells on day 1. (C) Area of Glioma on day 2. (D) The number of neuroblastoma cells divided by the area of glioma cells on day 2

Flat

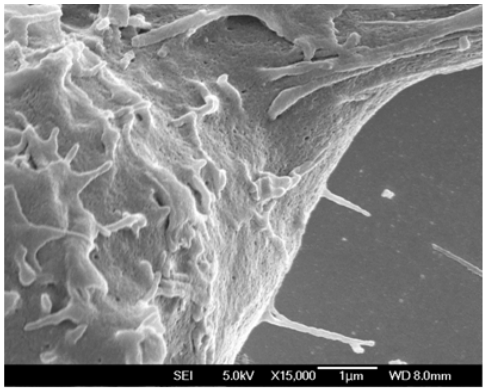

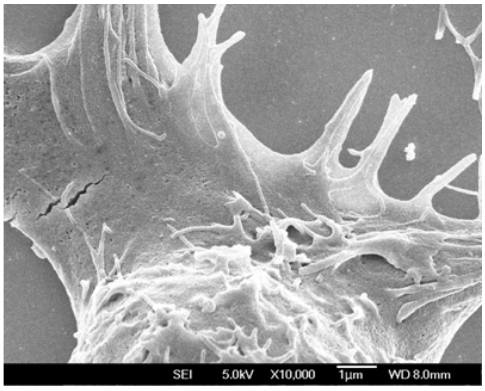

10nm

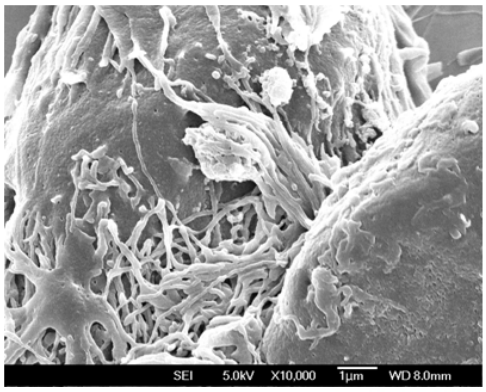

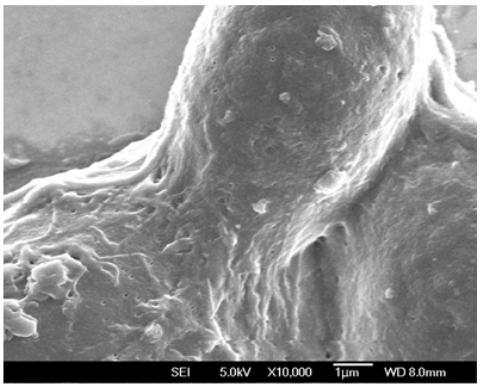

50nm

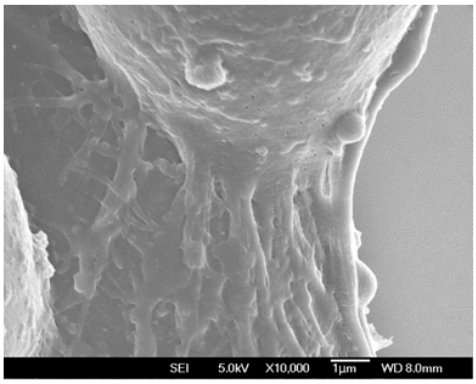

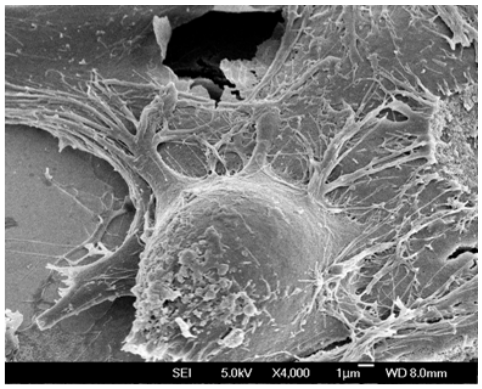

100nm

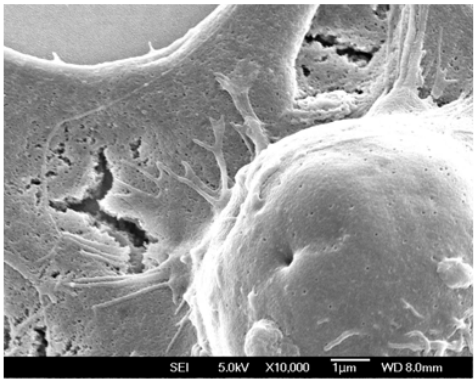

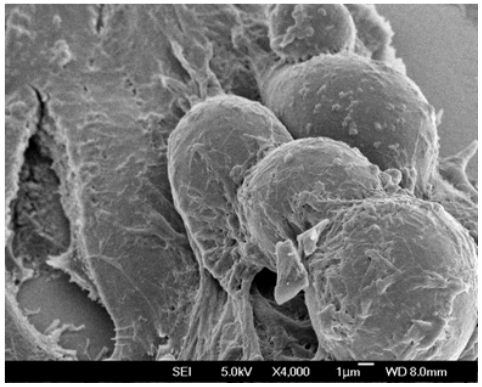

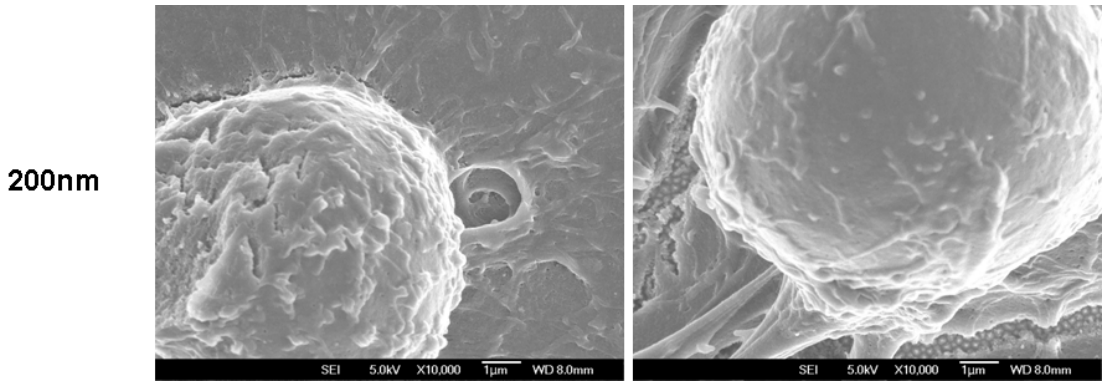

Figure 4. Filopodia of neuroblastoma cells on nanodot arrays on day 2.

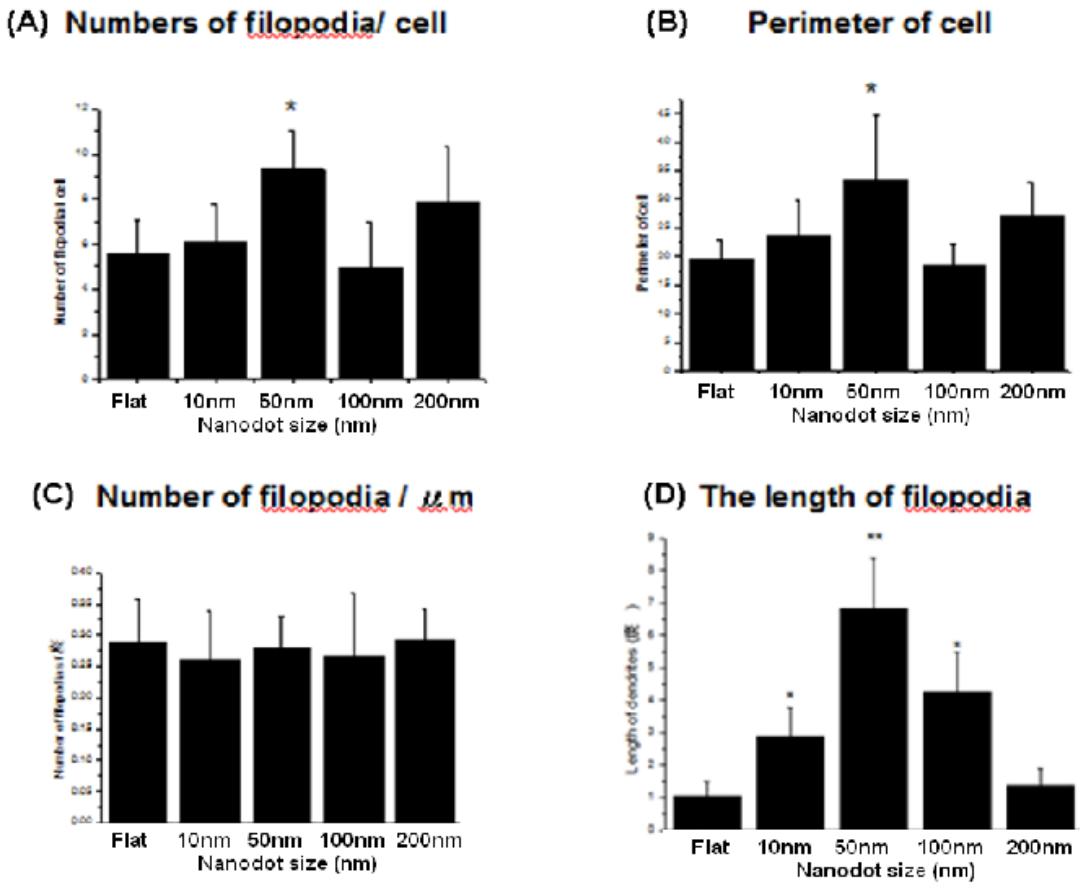

Figure 5. (A) Filopodia numbers of neuroblastoma cell (B) Perimeter of neuroblastoma (C) Filopodia number of neuroblastoma divided by perimeter (D) Filopodia length of neuroblastoma

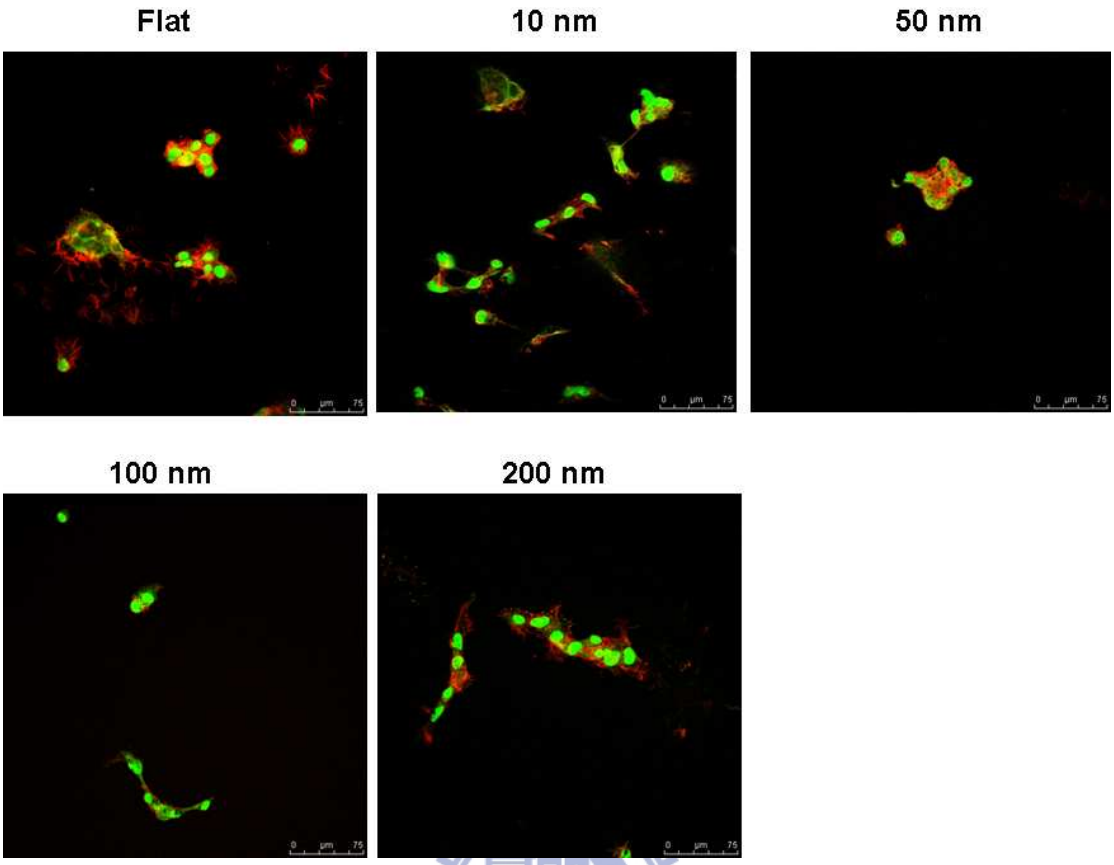

Figure 6. Confocal images of NG108-15 cells on different nanodat arrays. Green: Vinculin , Red: Phalloidin.

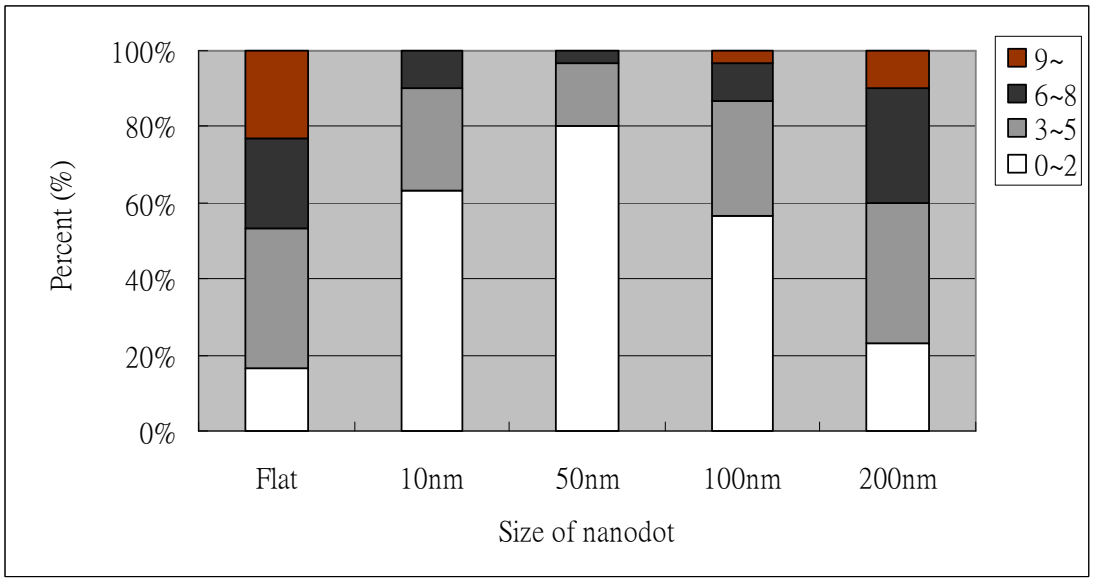

Figure 7. Percentage of glioma processes number distribution range on different sizes nanodot arrays.

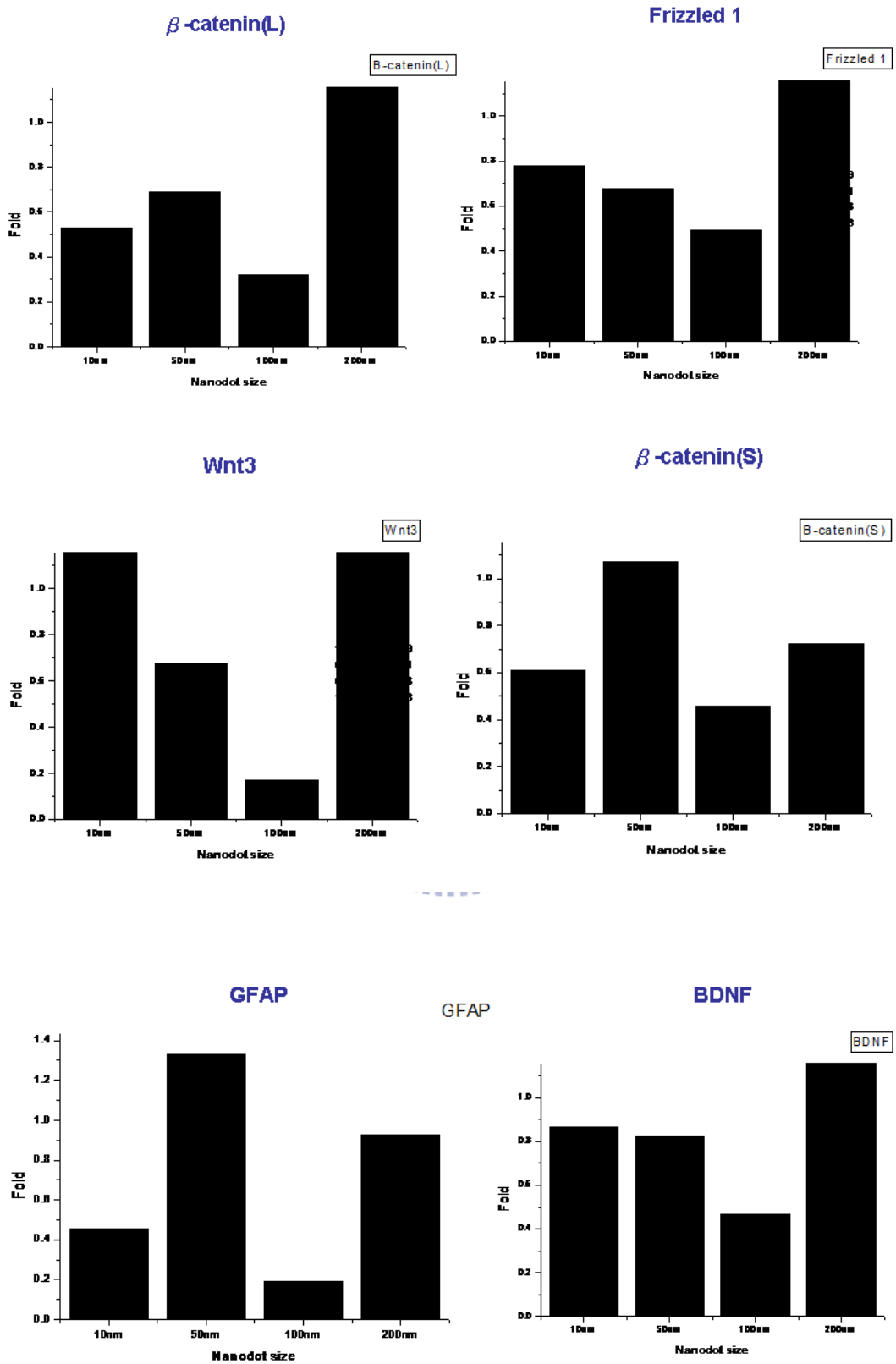

Figure 8. Fold change of each gene. We use GAPDH and flat surface as our control.

Reference

1. N. O. Glebova, D. D. Ginty, *Annu. Rev. Neurosci.* **28**, 191 (2005).
2. W. Qin, W. A. Bauman, C. Cardozo, *Annals of the New York Academy of Sciences* **1211**, 66 (2010).
3. K. D. Anderson, *Journal of neurotrauma* **21**, 1371 (2004).
4. J. H. Kim *et al.*, *Nature* **418**, 50 (2002).
5. M. Fava, K. S. Kendler, *Neuron* **28**, 335 (2000).
6. M. Goedert, M. Spillantini, R. Jakes, D. Rutherford, R. Crowther, *Neuron* **3**, 519 (1989).
7. A. M. Taylor *et al.*, *Nature methods* **2**, 599 (2005).
8. C. Chalfoun, G. Wirth, G. Evans, *Journal of Cellular and Molecular Medicine* **10**, 309 (2006).
9. M. Nedergaard, B. Ransom, S. A. Goldman, *TRENDS in Neurosciences* **26**, 523 (2003).
10. E. M. Ullian, K. S. Christopherson, B. A. Barres, *Glia* **47**, 209 (2004).
11. T. W. Wang, H. Zhang, J. M. Parent, *Development* **132**, 2721 (2005).
12. T. Ueki *et al.*, *The Journal of neuroscience* **23**, 11732 (2003).
13. J. P. Kaiser, A. Reinmann, A. Bruinink, *Biomaterials* **27**, 5230 (2006).
14. M. M. Stevens, J. H. George, *Science* **310**, 1135 (2005).
15. G. A. Silva *et al.*, *Science* **303**, 1352 (2004).
16. M. Schindler, I. Ahmed, J. Kamal, *Biomaterials* **26**, 5624 (2005).
17. E. Cukierman, R. Pankov, K. M. Yamada, *Current opinion in cell biology* **14**, 633 (2002).
18. V. Brunetti *et al.*, *Proceedings of the National Academy of Sciences* **107**, 6264 (2010).
19. E. Cavalcanti-Adam *et al.*, *Biophysical journal* **92**, 2964 (2007).
20. C. Choi, S. Hagvall, B. Wu, J. Dunn, R. Beygui, *Biomaterials* **28**, 1672 (2007).
21. F. Yang, R. Murugan, S. Wang, S. Ramakrishna, *Biomaterials* **26**, 2603 (2005).
22. B. Zhu *et al.*, *Biomaterials* **25**, 4215 (2004).
23. P. Wang, L. Li, C. Zhang, Q. Lei, W. Fang, *Biomaterials* **31**, 6201 (2010).
24. C. Xie *et al.*, *Nano Letters*, 273.
25. N. Fredin, A. Broderick, M. Buck, D. Lynn, *Biomacromolecules* **10**, 994 (2009).
26. S. Shankar, L. Rizzello, R. Cingolani, R. Rinaldi, P. Pompa, *ACS nano* **3**, 893 (2009).
27. F. Johansson, P. Carlberg, N. Danielsen, L. Montelius, M. Kanje, *Biomaterials*

27, 1251 (2006).
28. C. H. Choi *et al.*, *Biomaterials* **28**, 1672 (2007).
29. J. Park, S. Bauer, K. von der Mark, P. Schmuki, *Nano Letters* **7**, 1686 (2007).
30. Y. C. Hung, H. A. Pan, S. M. Tai, G. S. Huang, *Lab Chip* **10**, 1189 (2010).
31. C. T. Wu, F. H. Ko, H. Y. Hwang, *Microelectronic engineering* **83**, 1567 (2006).
32. D. Lie *et al.*, *NATURE-LONDON*- **7063**, 1370 (2005).
33. P. M. Lledo, M. Alonso, M. S. Grubb, *Nature Reviews Neuroscience* **7**, 179 (2006).
34. D. K. Ma, G. Ming, H. Song, *Current opinion in neurobiology* **15**, 514 (2005).
35. H. Scharfman *et al.*, *Experimental neurology* **192**, 348 (2005).
36. C. Rossi *et al.*, *European Journal of Neuroscience* **24**, 1850 (2006).
37. P. Mohapel, H. Frielingsdorf, J. Haggblad, O. Zachrisson, P. Brundin, *Neuroscience* **132**, 767 (2005).